Available online at www.sciencedirect.com

ScienceDirect

IFAC Papers Online CONFERENCE PAPER ARCHIVE

IFAC PapersOnLine 50-1 (2017) 7253–7259

Combined Singular Perturbations and Nonlinear Geometric Approach to FDI in Satellite Actuators and Sensors

P. Baldi [*,1] **P. Castaldi** [*] **N. Mimmo** [*] **S. Simani** [**]

[*] *Dipartimento di Ingegneria dell'Energia Elettrica e dell'Informazione, Università di Bologna, Facoltà di Ingegneria Aerospaziale. 47121 Forlì(FC), Italy. (e–mail: pietro.baldi2@unibo.it).*

[**] *Dipartimento di Ingegneria, Università di Ferrara. 44123 Ferrara (FE), Italy. (e–mail: silvio.simani@unife.it).*

Abstract: This paper presents a novel scheme for the detection and isolation of faults affecting the sensors measuring the satellite attitude, body angular velocity and flywheel spin rates as well as defects related to the control torques provided by satellite momentum wheels. Thanks to the jointly use of the singular perturbations theory and nonlinear geometric approach, a novel fault detection and isolation system has been developed to accurately detect and isolate faults occurring on all the considered actuators and sensors. Simulation results are based on a detailed nonlinear satellite model with embedded disturbance description. The results document the effectiveness of the proposed fault detection and isolation scheme.

Keywords: Fault detection and isolation, singular perturbations, nonlinear geometric approach, aerospace, actuators and sensors.

1. INTRODUCTION

The increasing operational requirements for onboard autonomy in satellite control systems require structural methods that support the design of complete and reliable supervisory systems. In this context, Fault Detection and Isolation (FDI) systems provide fundamental information about the system health status, to allow subsequent accommodation actions to improve system reliability and availability, while maintaining desirable performances.

Moreover, there has been a growing demand for methods guaranteeing fail safe operations with a reduced level of hardware redundancy. Hardware redundancy can be not available on small and low cost satellites, while a reduced level of hardware redundancy is useful also in large satellites and spacecrafts to avoid an increase of the system complexity, weights and costs.

Significant research in FDI has been done in the last decades (Isermann (2011); Blanke et al. (2016)). Numerous model-based methods have been proposed for fault diagnosis in linear and nonlinear systems (Chen-Patton (1999); Ding (2013); Bokor-Szabó (2009)). In particular, a solution to the FDI problem for nonlinear systems was presented in De Persis-Isidori (2001) through the NonLinear Geometric Approach (NLGA). The NLGA has been exploited by the authors of this paper also for the FDI in aircraft systems (Castaldi et al. (2010, 2014)), wind turbine systems (Simani-Castaldi (2014)) and in case of frequency faults in satellite actuators (Baldi et al. (2014)).

This paper presents a novel fault detection and isolation scheme to assess the health condition and proper functioning of essential sensors and actuators of a satellite Attitude Determination and Control Systems (ADCS).

This work is a development of a previous work of the same authors (Baldi et al. (2016)), which considered the presence of a redundant attitude sensor to perform the accurate isolation of all the actuator and sensor faults by exploiting the NLGA. In contrast, this paper exploits also the Singular Perturbations (SP) theory to define reduced order approximated models of the complete satellite model and allow the complete fault isolation without needing any hardware sensor redundancy.

The SP theory has been previously applied by some of the authors for the design of an Active Faut Tolerant Control (AFTC) system for civil aircrafts (Castaldi et al. (2013)). The SP theory results to be a very advantageous framework to describe the dynamics of systems characterised by different time scales (Khalil (2002)). The joint use of the NLGA and SP theory represents a peculiar aspect of the proposed approach and allows to take advantage of the benefits of both of them, thus resulding in a novel and reliable FDI system.

Each physical sensor fault has been mapped to a set of (always simultaneous) *mathematical* additive fault inputs as described in Mattone-De Luca (2006). This allows the definition of a nonlinear model affine in all the actuator and sensor fault inputs, with a structure suitable for the application of the NLGA (see De Persis-Isidori (2001)) to obtain the FDI of both actuator and sensor faults.

The FDI residual filters are designed via the NLGA to obtain diagnostic signals that are sensitive to specific subsets of actuator and sensor faults and decoupled from the remaining ones. The fault isolation task is achieved, with the assumption of single fault occurring at any time, through a residual cross-check scheme and a proper decision logic.

[1] Corresponding author.

10.1016/j.ifacol.2017.08.1375

The FDI performances has been evaluated using a detailed nonlinear satellite simulator taking account also of gyroscopic effects, measurement noise and exogenous disturbance signals. Simulation results are given in case of both actuator and sensor faults, validating the ability of the proposed scheme to deal with faults of different types and provide an accurate fault detection and isolation.

2. SATELLITE AND ACTUATOR MODELS

The satellite is considered as a rigid body, whose attitude is represented by using the quaternion notation. The satellite mathematical model is given by the dynamic and kinematic equations of (1) and (2) (Wie (2008)):

$$\dot{\omega} = -\mathbf{I}_s^{-1}\mathbf{S}(\omega)(\mathbf{I}_s\omega + \mathbf{h}_{rw}) + \mathbf{I}_s^{-1}(\mathbf{M}_{sat} + \mathbf{M}_{ext}) \quad (1)$$

$$\dot{\mathbf{q}} = \frac{1}{2}\mathbf{\Omega}(\omega)\mathbf{q} \quad (2)$$

with $\mathbf{M}_{ext} = \mathbf{M}_{gg} + \mathbf{M}_{aero}$, the skew-symmetric matrices

$$\mathbf{S}(\omega) = \begin{bmatrix} 0 & -\omega_3 & \omega_2 \\ \omega_3 & 0 & -\omega_1 \\ -\omega_2 & \omega_1 & 0 \end{bmatrix}, \mathbf{\Omega}(\omega) = \begin{bmatrix} 0 & \omega_3 & -\omega_2 & \omega_1 \\ -\omega_3 & 0 & \omega_1 & \omega_2 \\ \omega_2 & -\omega_1 & 0 & \omega_3 \\ -\omega_1 & -\omega_2 & -\omega_3 & 0 \end{bmatrix} \quad (3)$$

and where $\omega = [\omega_1, \omega_2, \omega_3]^T$ is the vector of the roll, pitch and yaw body rates, $\mathbf{q} = [q_1, q_2, q_3, q_4]^T$ is the quaternion vector and $\mathbf{h}_{rw} = [h_{rw1}, h_{rw2}, h_{rw3}, h_{rw4}]^T$ is the vector of the flywheel angular momenta. The principal inertia body-fixed frame is considered, with I_{xx}, I_{yy}, and I_{zz} on the main diagonal of the satellite inertia matrix $\mathbf{I}_s$. Moreover, it is assumed that $I_{xx} > I_{yy}, I_{zz}$ and $I_{yy} \approx I_{zz}$.
The considered Attitude Control System (ACS) consists of a fixed array of three orthogonal momentum wheels mounted along the satellite body axes. The elements of the vector $\mathbf{M}_{sat} = [M_{sat_1}, M_{sat_2}, M_{sat_3}]^T$ are the control torques provided by the momentum wheels for active 3-axis attitude control. Equation (1) explicitly includes the gravitational and aerodynamic disturbance torques $\mathbf{M}_{gg}$ and $\mathbf{M}_{aero}$ about the centre of mass. These disturbances typically represent the most important external disturbance torques affecting Low Earth Orbit (LEO) satellites (Wie (2008)). The gravity gradient torque $\mathbf{M}_{gg}$ is

$$\mathbf{M}_{gg} = \frac{3\mu}{R^3}(\hat{v}_{nadir} \times I_s\hat{v}_{nadir}) \quad (4)$$

where μ and R are the gravitational constant and the orbit radius, respectively, and $\hat{v}_{nadir}$ is the unit vector towards nadir expressed in body-frame coordinates. The aerodynamic torque $\mathbf{M}_{aero}$ is

$$\mathbf{M}_{aero} = \frac{1}{2}\rho S_p V^2 C_D(\hat{v}_V \times \mathbf{r}_{cp}) \quad (5)$$

where ρ is the atmospheric density, V is the relative velocity of the satellite, S_p is the reference area affected by the aerodynamic flux, and C_D is the drag coefficient. $\mathbf{r_{cp}} = \left[r_{x_{cp}}, r_{y_{cp}}, r_{z_{cp}}\right]^T$ is the vector joining the centre of mass and the aerodynamic centre of pressure and $\hat{v}_V$ is the unit velocity vector expressed in body-frame coordinates. The dynamic equations of the momentum wheels are

$$\dot{\omega}_{rw} = {J_{rw}}^{-1}\dot{\mathbf{h}}_{rw} = {J_{rw}}^{-1}(\mathbf{M}_{rw} - b\,\omega_{rw} - c\;sgn(\omega_{rw})) \quad (6)$$

where J_{rw} is the flywheel inertia, $\mathbf{h}_{rw} = J_{rw}\omega_{rw}$ is the the flywheel angular momenta vector, $\omega_{rw} = [\omega_{rw_1}, \omega_{rw_2}, \omega_{rw_3}]^T$ is the flywheel spin rates vector and b, c are the viscous and Coulomb friction coefficients, respectively (Carrara et al. (2012)). The elements of the input vector $\mathbf{M}_{rw} = [M_{rw_1}, M_{rw_2}, M_{rw_3}]^T$ are the torques provided by the actuator motors to control the flywheel spin rates. The attitude control torques acting on the satellite can be defined as

$$\mathbf{M}_{sat} = -J_{rw}\dot{\omega}_{rw} = -\mathbf{M}_{rw} + b\,\omega_{rw} + c\;sgn(\omega_{rw}) \quad (7)$$

The state vector of the overall system model (1), (2), (6) is $\mathbf{x} = [\omega_1, \omega_2, \omega_3, \mathbf{q}, \omega_{rw_1}, \omega_{rw_2}, \omega_{rw_3}]^T$ and all the state variables are assumed to be measurable. The actual input vector of the overall system is $\mathbf{u} = [M_{rw_1}, M_{rw_2}, M_{rw_3}]^T$.

3. FAULT DETECTION AND ISOLATION

3.1 Singular Perturbations Theory Applied to FDI

Here a brief introduction of the SP theory is given. For a comprehensive description refer to Khalil (2002).
The actual dynamics of a generic system characterised by two different time scales (*i.e.* a slow and a fast dynamics) can be expressed in terms of fast and slow variables:

$$\begin{cases} \dot{\mathbf{x}}_1 = \mathbf{n}_1(\mathbf{x}_1, \mathbf{x}_2, \varepsilon) + \mathbf{g}_1(\mathbf{x}_1, \mathbf{x}_2, \varepsilon)\mathbf{u} \\ \varepsilon\dot{\mathbf{x}}_2 = \mathbf{n}_2(\mathbf{x}_1, \mathbf{x}_2, \varepsilon) + \mathbf{g}_2(\mathbf{x}_1, \mathbf{x}_2, \varepsilon)\mathbf{u} \end{cases} \quad (8)$$

where $\mathbf{x}_1 \in \mathbb{R}^{n_1}$ is the vector of slow variables, $\mathbf{x}_2 \in \mathbb{R}^{n_2}$ is the vector of fast ones, $\mathbf{u} \in \mathbb{R}^p$ is the input vector. ε is the small perturbation parameter satisfying $0 < \varepsilon \ll 1$.
Considering also the presence of additive actuator and sensor faults, the singularly perturbed system can be written as

$$\begin{cases} \dot{\mathbf{x}}_1 = \mathbf{n}_1(\mathbf{x}_1, \mathbf{x}_2, \varepsilon) + \mathbf{g}_1(\mathbf{x}_1, \mathbf{x}_2, \varepsilon)\left[\mathbf{u}_c + \mathbf{F}_u\right] \\ \varepsilon\dot{\mathbf{x}}_2 = \mathbf{n}_2(\mathbf{x}_1, \mathbf{x}_2, \varepsilon) + \mathbf{g}_2(\mathbf{x}_1, \mathbf{x}_2, \varepsilon)\left[\mathbf{u}_c + \mathbf{F}_u\right] \end{cases} \quad (9)$$

The terms $\mathbf{F}_{\mathbf{x}_1}$, $\mathbf{F}_{\mathbf{x}_2}$ and $\mathbf{F}_u$ represent the additive fault vectors acting on sensor outputs and actuator inputs:

$$\mathbf{y}_1 = \mathbf{x}_1 + \mathbf{F}_{\mathbf{x}_1} \qquad \mathbf{y}_2 = \mathbf{x}_2 + \mathbf{F}_{\mathbf{x}_2} \qquad \mathbf{u} = \mathbf{u}_c + \mathbf{F}_u \quad (10)$$

where $\mathbf{y}_1$, $\mathbf{y}_2$, $\mathbf{u}$, $\mathbf{u}_c$ represent the slow variable output, the fast variable output, the actual actuator input and the commanded actuator input, respectively. Let's denote with n the number of physical faults affecting sensors ($n = n_1 + n_2$), while p is the number of actuator faults.
By assuming $\varepsilon = 0$ the state-space dimension reduces from n_1+n_2 to n_1 because the second relation in (9) degenerates to an algebraic equation:

$$\begin{cases} \dot{\bar{\mathbf{x}}}_1 = \mathbf{n}_1(\bar{\mathbf{x}}_1, \bar{\mathbf{x}}_2, 0) + \mathbf{g}_1(\bar{\mathbf{x}}_1, \bar{\mathbf{x}}_2, 0)\left[\mathbf{u}_c + \mathbf{F}_u\right] \\ 0 = \mathbf{n}_2(\bar{\mathbf{x}}_1, \bar{\mathbf{x}}_2, 0) + \mathbf{g}_2(\bar{\mathbf{x}}_1, \bar{\mathbf{x}}_2, 0)\left[\mathbf{u}_c + \mathbf{F}_u\right] \end{cases} \quad (11)$$

Equations (11) represent the *reduced model*. If $\mathbf{x}_{2_\mathcal{M}} = \bar{\mathbf{x}}_2 = \mathbf{h}(\bar{\mathbf{x}}_1, \mathbf{u}_c + \mathbf{F}_u)$ is an isolate root of $0 = \mathbf{n}_2(\bar{\mathbf{x}}_1, \mathbf{x}_2, 0) + \mathbf{g}_2(\bar{\mathbf{x}}_1, \mathbf{x}_2, 0)\left[\mathbf{u}_c + \mathbf{F}_u\right]$ satisfing the Tikhonov's theorem also in case of faults, then it describes a $n_1 + p$ dimension invariant manifold for the system (11) (Khalil (2002)).
Thanks to a time scale change, made by defining $\tau = (t - t_0)/\varepsilon$, apex derivative can be defined as $\mathbf{x}' = d\mathbf{x}/d\tau$. Again, by assuming $\varepsilon = 0$, the dynamic order of the system is reduced from $n_1 + n_2$ to n_2 and equations (12) represent the *boundary–layer model*:

$$\begin{cases} \mathbf{x}_1' = 0 \\ \mathbf{x}_2' = \mathbf{n}_2(\mathbf{x}_1, \mathbf{x}_2, 0) + \mathbf{g}_2(\mathbf{x}_1, \mathbf{x}_2, 0)\left[\mathbf{u}_c + \mathbf{F}_u\right] \end{cases} \quad (12)$$

Finally, if Tikhonov's theorem is verified, the actual system dynamics (9) can be approximated by its reduced and boundary layer models:

$$\begin{cases} \dot{\bar{\mathbf{x}}}_1 = \mathbf{n}_1(\bar{\mathbf{x}}_1, \mathbf{h}(\bar{\mathbf{x}}_1, \mathbf{u}_c + \mathbf{F}_u), 0) + \\ \qquad +\mathbf{g}_1(\bar{\mathbf{x}}_1, \mathbf{h}(\bar{\mathbf{x}}_1, \mathbf{u}_c + \mathbf{F}_u), 0)\,[\mathbf{u}_c + \mathbf{F}_u] \\ \mathbf{x}_2' = \mathbf{n}_2(\bar{\mathbf{x}}_1, \mathbf{x}_2, 0) + \mathbf{g}_2(\bar{\mathbf{x}}_1, \mathbf{x}_2, 0)\,[\mathbf{u}_c + \mathbf{F}_u] \end{cases} \tag{13}$$

Rewriting the dynamics of (9) in terms of output variables, it can be seen that the resulting model (14) is not affine with respect to sensor faults:

$$\begin{cases} \dot{\mathbf{y}}_1 = \mathbf{n}_1(\mathbf{y}_1 - \mathbf{F}_{\mathbf{x}_1}, \mathbf{y}_2 - \mathbf{F}_{\mathbf{x}_2}, \varepsilon) + \\ \qquad +\mathbf{g}_1(\mathbf{y}_1 - \mathbf{F}_{\mathbf{x}_1}, \mathbf{y}_2 - \mathbf{F}_{\mathbf{x}_2}, \varepsilon)\,[\mathbf{u}_c + \mathbf{F}_u] + \dot{\mathbf{F}}_{\mathbf{x}_1} \\ \varepsilon\dot{\mathbf{y}}_2 = \mathbf{n}_2(\mathbf{y}_1 - \mathbf{F}_{\mathbf{x}_1}, \mathbf{y}_2 - \mathbf{F}_{\mathbf{x}_2}, \varepsilon) + \\ \qquad +\mathbf{g}_2(\mathbf{y}_1 - \mathbf{F}_{\mathbf{x}_1}, \mathbf{y}_2 - \mathbf{F}_{\mathbf{x}_2}, \varepsilon)\,[\mathbf{u}_c + \mathbf{F}_u] + \varepsilon\dot{\mathbf{F}}_{\mathbf{x}_2} \end{cases} \tag{14}$$

A different modelling procedure for sensor faults was proposed by Mattone-De Luca (2006) to obtain a dynamic model suitable for the NLGA with a structure affine in all the fault inputs. $\nu_k \geq 1$ always simultaneous *mathematical* fault inputs $f_{x_k,i} (i = 1, ..., \nu_k)$ are introduced in place of the physical fault $F_{x_k}\ \forall k \in \{1, ..., n\}$, including also a fault input associated to the time derivative of the fault. Whenever a physical sensor fault occurs, *i.e.* $F_{x_k} \neq 0$, all associated mathematical faults $f_{x_k,i} (i = 1, ..., \nu_k)$ will become generically nonzero, although with different time behaviors and, in general, without a direct physical interpretation. Therefore, it will be sufficient to recognise the occurrence of *any* (one or more) of the associated mathematical fault inputs. For a comprehensive description of this modelling procedure refer to Mattone-De Luca (2006).
Hence, the system dynamics subject to actuator and sensor faults can be written in terms of output variables as

$$\begin{cases} \dot{\mathbf{y}}_1 = \mathbf{n}_1(\mathbf{y}_1, \mathbf{y}_2, \varepsilon) + \mathbf{g}_1(\mathbf{y}_1, \mathbf{y}_2, \varepsilon)\mathbf{u}_c + \\ \qquad + \sum_{k=1}^{n+p} \sum_{i=1}^{\nu_k} \mathbf{l}_{1_{x_k,i}}(\mathbf{y}_1, \mathbf{y}_2, \varepsilon) f_{x_k,i} \\ \varepsilon\dot{\mathbf{y}}_2 = \mathbf{n}_2(\mathbf{y}_1, \mathbf{y}_2, \varepsilon) + \mathbf{g}_2(\mathbf{y}_1, \mathbf{y}_2, \varepsilon)\mathbf{u}_c + \\ \qquad + \sum_{k=1}^{n+p} \sum_{i=1}^{\nu_k} \mathbf{l}_{2_{x_k,i}}(\mathbf{y}_1, \mathbf{y}_2, \varepsilon) f_{x_k,i} \end{cases} \tag{15}$$

where the terms $\mathbf{l}_{1_{x_k,i}}$ and $\mathbf{l}_{2_{x_k,i}}$ represent the input distributions of mathematical sensor and actuator faults. If the following necessary and sufficient conditions are satisfied for all physical faults, then the FDI problem can be solved for model (15) (Mattone-De Luca (2006)):

$$\begin{array}{rl} & \forall k, \forall i \neq k, \exists j \in \{1, ..., \nu_k\} : span\{\mathbf{l}_{x_k,j}\} \nsubseteq \bar{P}_i \\ OR & \forall k, \forall i \neq k, \exists h \in \{1, ..., \nu_i\} : span\{\mathbf{l}_{x_i,h}\} \nsubseteq \bar{P}_k \end{array} \tag{16}$$

with $\bar{P}_i$ involutive closure of $P_i = span\{\mathbf{l}_{x_i,1}, ..., \mathbf{l}_{x_i,\nu_i}\}$. The terms $\mathbf{l}_{x_k,j}$ are the mathematical fault input distributions for the overall system, *i.e.* $\mathbf{l}_{x_k,j} = \left[\mathbf{l}_{1x_k,j}^T, \mathbf{l}_{2x_k,j}^T\right]^T$. Since the input distributions of (15) are determined by the physical system model, the FDI problem could have no solution for the structure of (15) due to the possible unisolability of some actuator or sensor faults. However, using this mapping procedure for both actuator and sensor faults, the SP approximated dynamics of the generic system (13) in terms of output variables can be derived, where n_1 is the dimension of the slow state $\mathbf{x}_1$:

$$\begin{cases} \dot{\mathbf{y}}_1 = \mathbf{n}_1(\mathbf{y}_1, \mathbf{h}(\mathbf{y}_1, \mathbf{u}_c), 0) + \\ \qquad +\mathbf{g}_1(\mathbf{y}_1, \mathbf{h}(\mathbf{y}_1, \mathbf{u}_c), 0)\mathbf{u}_c + \\ \qquad + \sum_{k=1}^{n_1+p} \sum_{i=1}^{\nu_k} \mathbf{l}_{1_{x_k,i}}(\mathbf{y}_1) f_{x_k,i} \\ \mathbf{y}_2' = \mathbf{n}_2(\mathbf{y}_1, \mathbf{y}_2, 0) + \mathbf{g}_2(\mathbf{y}_1, \mathbf{y}_2, 0)\mathbf{u}_c + \\ \qquad + \sum_{k=1}^{n+p} \sum_{i=1}^{\nu_k} \mathbf{l}_{2_{x_k,i}}(\mathbf{y}_1, \mathbf{y}_2) f_{x_k,i} \end{cases} \tag{17}$$

Thanks to SP model approximations, the FDI problem can be solved for the structure of system (17), *i.e.* the conditions (16) are satisfied, and thus each of the non simultaneous physical faults can be detected and isolated.

3.2 Actuator and Sensor Fault Modelling

Possible faults affecting the actuated wheel motor torques, flywheel spin rate, satellite attitude and angular velocity measurements are considered and it is assumed that at most one fault affects the system at any time:

$$\begin{array}{ll} F_{Mi} = f_{Mi} = M_{rw_i} - M_{rw_{c,i}} & (i = 1, ..., 3) \\ F_{\omega_{rw_j}} = \omega_{rw_{y,j}} - \omega_{rw_j} & (j = 1, ..., 3) \\ F_{\omega_l} = \omega_{y,l} - \omega_l & (l = 1, ..., 3) \\ F_{q_m} = q_{y,m} - q_m & (m = 1, ..., 4) \end{array} \tag{18}$$

where $M_{rw_{c,i}}$ is the commanded control input and the sensor faults are defined as the differences between the real values ω_{rw_j}, ω_l, q_m and measured values $\omega_{rw_{y,j}}$, $\omega_{y,l}$, $q_{y,m}$. Physical attitude sensor faults generally affect all the quaternion components simultaneously, thus an attitude sensor fault is thereafter modelled as a single additive fault vector $\mathbf{F_q} = [F_{q_1}, F_{q_2}, F_{q_3}, F_{q_4}]^T$.
If (1), (2) and (6) are rewritten by considering the sensor outputs $\omega_{rw_{y,j}} = \omega_{rw_j} + F_{\omega_{rw_j}}$, $\omega_{y,l} = \omega_l + F_{\omega_l}$, $q_{y,m} = q_m + F_{q_m}$ (*i.e.* $y = x + F_x$) as new state variables, the general structure of a nonlinear system for the NLGA, which is affine in both the actuator and sensor fault inputs is recovered using the fault mapping procedure proposed by Mattone-De Luca (2006) and summarised in Section 3.1.

3.3 Nonlinear Geometric Approach

The NLGA was formally developed by De Persis-Isidori (2001), and it relies on a coordinate change in the state and output spaces providing an observable subsystem which, if it exists, is affected by the fault (or faults) to be detected, but unaffected by any other fault to be decoupled. In the new (local) coordinates, the system can be decomposed into three subsystems $\tilde{x}_1$, $\tilde{x}_2$ and $\tilde{x}_3$, where $\tilde{x}_1$ is the measured part of the state affected only by the fault term f to be detected, whilst $\tilde{x}_2$ and $\tilde{x}_3$ represent the measured and not measured part of the state affected by all the faults and disturbances, respectively. For a comprehensive description of the NLGA refer to De Persis-Isidori (2001). Denoting $\tilde{x}_2$ with $\tilde{y}_2$ and considering it as an independent input, the $\tilde{x}_1$-subsystem can be defined as follows:

$$\begin{cases} \dot{\tilde{x}}_1 = n_1(\tilde{x}_1, \tilde{y}_2) + g_1(\tilde{x}_1, \tilde{y}_2)\,u_c + \ell_1(\tilde{x}_1, \tilde{y}_2, \tilde{x}_3)\,f \\ \tilde{y}_1 = h(\tilde{x}_1) \end{cases} \tag{19}$$

with $\ell_1(\tilde{x}_1, \tilde{y}_2, \tilde{x}_3) \neq 0$. Starting from (19), a generic residual generator in filter form is modelled as follows:

$$\begin{cases} \dot{\xi} = n_1(\tilde{y}_1, \tilde{y}_2) + g_1(\tilde{y}_1, \tilde{y}_2)\,u_c + L(\tilde{y}_1 - \xi) \\ r = \tilde{y}_1 - \xi \end{cases} \tag{20}$$

where $L > 0$ is the gain of the asymptotically stable residual filter and r is the generated diagnostic signal.

3.4 SP Approximated Satellite and Actuator Dynamics

Considering the equations of the actuator and satellite dynamics (6) and (2), the vector of the slow variables $\mathbf{x}_1 = [\omega_1, \omega_2, \omega_3, q_1, q_2, q_3, q_4]^T$, the vector of the fast variables $\mathbf{x}_2 = [\omega_{rw_1}, \omega_{rw_2}, \omega_{rw_3}]^T$ and the perturbation parameter $\varepsilon_1 = J_{rw}$ can be defined considering the flywheel dynamics to be faster than the satellite one. Since $J_{rw} << 1$, the following SP approximated satellite dynamic model can be defined and exploited for the NLGA application, by applying the SP theory described in Section 3.1:

$$\begin{aligned}
\dot{\omega}_1 &= -\frac{(J_{zz} - J_{yy})}{J_{xx}}\omega_2\omega_3 + \frac{M_{gg_x}}{J_{xx}} + \frac{M_{aero_x}}{J_{xx}} \\
\dot{\omega}_2 &= -\frac{(J_{xx} - J_{zz})}{J_{yy}}\omega_1\omega_3 + \frac{M_{gg_y}}{J_{yy}} + \frac{M_{aero_y}}{J_{yy}} \\
\dot{\omega}_3 &= -\frac{(J_{yy} - J_{xx})}{J_{zz}}\omega_1\omega_2 + \frac{M_{gg_z}}{J_{zz}} + \frac{M_{aero_z}}{J_{zz}}
\end{aligned} \tag{21}$$

with the invariant manifold $\mathbf{x}_{2M}$ for the reduced system defined by

$$\begin{bmatrix} \omega_{rw_{1M}} \\ \omega_{rw_{2M}} \\ \omega_{rw_{3M}} \end{bmatrix} = \begin{bmatrix} \frac{M_{rw_1} - c\,sgn(\omega_{rw})}{b} \\ \frac{M_{rw_2} - c\,sgn(\omega_{rw})}{b} \\ \frac{M_{rw_3} - c\,sgn(\omega_{rw})}{b} \end{bmatrix} \tag{22}$$

It is worth noting that the SP approximated dynamic model of the satellite describes an autonomous system without manipulable inputs and independent also from the fast variables.

3.5 NLGA Filters for Actuator and Flywheel Sensor FDI

The NLGA FDI system is designed on the basis of the input affine nonlinear model structure (15) as described in (De Persis-Isidori (2001); Baldi et al. (2016)). Since the flywheel spin rate measurements are assumed to be available, it is straightforward to design three simple scalar NLGA residual filters independent of the satellite attitude and angular velocity, and exploiting information provided only by the momentum wheel sensors, directly on the basis of (6). Each of these NLGA residual filters results to be sensitive only to the couple of faults f_{M_i}, $f_{\omega_{rw_{j,1}}} = F_{\omega_{rw_j}}$ $(i = j)$, *i.e.* the actuator and flywheel spin rate sensor faults related to the same i-th momentum wheel, respectively, and the fault input $f_{\omega_{rw_{j,5}}} = \dot{F}_{\omega_{rw_j}}$, *i.e.* the time derivative of the physical sensor fault. The scalar state variables ξ of these three NLGA residual filters are

$$\xi_1 = J_{rw}\omega_{rw_1}/b \quad \xi_2 = J_{rw}\omega_{rw_2}/b \quad \xi_3 = J_{rw}\omega_{rw_3}/b \tag{23}$$

where $h_j = J_{rw}\omega_{rw_j}$ $(j = 1, ..., 4)$ are the measured angular momenta of the three flywheels, J_{rw} is the flywheel inertia and b is the viscous friction coefficient. These three filters allow the isolation of the momentum wheel subsystem affected by a possible actuator or flywheel spin rate sensor fault, but not the complete fault isolation.
Additional NLGA residual filters can be designed to allow the complete isolation of a detected fault. On the basis of the SP approximated model of the satellite dynamics (21), other three simple NLGA scalar residual filters can be designed and their scalar state variables ξ are

$$\xi_4 = J_{xx}\omega_1 \qquad \xi_5 = J_{yy}\omega_2 \qquad \xi_6 = J_{zz}\omega_3 \tag{24}$$

It is worth noting that, since the SP reduced dynamic model (21) represents an autonomous system without manipulable inputs, the three obtained residuals result to be sensitive to any actuator fault when the actual satellite angular velocities change due to an actuator fault.

3.6 SP Approximated Satellite Dynamics and Kinematics

Considering the equations of the satellite dynamics and kinematics (1) and (2), the vector of the slow variables can be defined as $\mathbf{x}_1 = [\omega_1, q_1, q_2, q_3, q_4, h_{rw_1}, h_{rw_2}, h_{rw_3}]^T$ with $\mathbf{h}_{rw} = J_{rw}\boldsymbol{\omega}_{rw}$, and the vector of the fast variables as $\mathbf{x}_2 = [\omega_2, \omega_3]^T$ by defining a second perturbation parameter $\varepsilon_2 = J_{zz}/J_{xx} \approx J_{yy}/J_{xx} < 1$ since it has been assumed that $I_{xx} > I_{yy}, I_{zz}$ and $I_{yy} \approx I_{zz}$. Thanks to this assumption, the dynamics of ω_2, ω_3 are considered to be faster than the one of ω_1. The following SP approximated satellite kinematic model can be defined, by applying the SP theory described in Section 3.1:

$$\begin{aligned}
\dot{q}_1 &= \frac{1}{2}\left(\omega_1 q_4 - \omega_{2M} q_3 + \omega_{3M} q_2\right) \\
\dot{q}_2 &= \frac{1}{2}\left(\omega_1 q_3 + \omega_{2M} q_4 - \omega_{3M} q_1\right) \\
\dot{q}_3 &= \frac{1}{2}\left(-\omega_1 q_2 + \omega_{2M} q_1 + \omega_{3M} q_4\right) \\
\dot{q}_4 &= \frac{1}{2}\left(-\omega_1 q_1 - \omega_{2M} q_2 - \omega_{3M} q_3\right)
\end{aligned} \tag{25}$$

with the invariant manifold $\mathbf{x}_{2M}$ for the reduced system defined by

$$\begin{bmatrix} \omega_{2M} \\ \omega_{3M} \end{bmatrix} = \begin{bmatrix} \frac{M_{rw_3} - b\omega_{rw_3} - csign(\omega_{rw_3}) - M_{ext_z} + \omega_1 h_{rw_2}}{J_{xx}\omega_1 + h_{rw_1}} \\ \frac{-M_{rw_2} + b\omega_{rw_2} + csign(\omega_{rw_2}) + M_{ext_y} + \omega_1 h_{rw_3}}{J_{xx}\omega_1 + h_{rw_1}} \end{bmatrix} \tag{26}$$

where $\mathbf{M}_{ext} = \mathbf{M}_{gg} + \mathbf{M}_{aero}$. It is worth noting that an isolated solution for the manifold can be guaranteed for a 3-axis stabilised satellite with a null or very low angular velocity thanks to the use of momentum wheels spinning at a sufficiently high nominal spin rate.

3.7 NLGA Filters for Attitude and Angular Velocity Sensor FDI

Starting from the exact kinematic model (2) of the satellite, a set of nine scalar NLGA residual filters organised as a *generalised scheme* is designed to detect and isolate the occurrence of possible faults $\mathbf{F_q}$ and F_{ω_l} $(l = 1, ..., 3)$. Thanks to the NLGA, each of these residual filters results to be sensitive only to a couple of physical angular velocity sensor faults F_{ω_l} $(l = 1, ..., 3)$ and to the physical attitude sensor fault $\mathbf{F_q}$ through the associated mathematical fault inputs. The scalar state variables ξ of the nine designed NLGA residual filters are

$$\begin{array}{lll}
\xi_7 = 1 - 2q_2^2 - 2q_3^2 & \xi_{10} = 1 - 2q_1^2 - 2q_3^2 & \xi_{13} = 1 - 2q_1^2 - 2q_2^2 \\
\xi_8 = 2(q_1q_2 + q_3q_4) & \xi_{11} = 2(q_1q_3 + q_2q_4) & \xi_{14} = 2(q_1q_2 - q_3q_4) \\
\xi_9 = 2(q_1q_4 + q_2q_3) & \xi_{12} = 2(q_1q_3 - q_2q_4) & \xi_{15} = 2(q_2q_3 - q_1q_4)
\end{array} \tag{27}$$

Moreover, an additional set of nine scalar NLGA residual filters organised as a *generalised scheme* is designed

starting from the SP approximated model (25) of the satellite kinematics derived in Section 3.6. The scalar state variables ξ of these nine additional NLGA residual filters are the same of (27). However, since the equations of the SP approximated kinematic model results to be functions only of the assumed slow variables $\mathbf{q}$ and ω_1 (in addition to the slow variables $\mathbf{h}_{rw}$ and inputs M_{rw_2}, M_{rw_3} entering through the expressions of the manifold variables), each of these nine residual filters results to be sensitive to the physical angular velocity sensor fault F_{ω_1} and only to the physical attitude sensor fault $\mathbf{F_q}$ (in addition to the faults affecting $\mathbf{h}_{rw}$, M_{rw_2}, M_{rw_3}) through the associated mathematical fault inputs. Therefore, since the two designed sets are both sensitive to possible faults $\mathbf{F_q}$ on the attitude sensor and F_{ω_1} on the first satellite angular velocity sensor, whilst only the first set is sensitive to possible faults F_{ω_2}, F_{ω_3} on the other two angular velocity sensors, it is possible to achieve an accurate isolation of attitude and angular velocity faults through a proper decision logic and a crosscheck of the residuals of these two sets.

3.8 Residual Cross-check Scheme for FDI

Assuming a single fault at any time, possible faults affecting the actuated torques or the flywheel spin rate measurements can be detected and isolated by cross-checking the six residuals $r_1, ..., r_6$ of the NLGA filters based on the variables (23) and (24) described in Section 3.5:

(1) Firstly, the three residuals $r_1, ..., r_3$ derived from the exact actuator dynamic model (6), which are sensitive only to actuator and sensor faults affecting a specific momentum wheel, are analyzed. Thus, the faulty actuator subsystem can be detected and isolated.
(2) Then, the three residuals $r_4, ..., r_6$ derived from the SP approximated satellite dynamic model (21), which are sensitive only to actuator faults and insensitive to flywheel spin rate sensor faults, are checked to precisely recognise the occurred fault type.

On the other hand, possible faults affecting the satellite angular velocity or attitude measurements can be detected and isolated by cross-checking the two sets of nine residuals $r_{7,n}, ..., r_{15,n}$, $(n = 1, 2)$ of the NLGA filters based on the variables (27) described in Section 3.7 and derived from the exact satellite kinematic model (2) and SP approximated kinematic model (25), respectively, as follows:

(1) Firstly, the corresponding residuals of the two sets are compared. Since each set exploits the measurements of the same attitude sensor and different angular velocity sensors, the two sets show the same residual behaviours only in case of attitude sensor faults and different residual behaviours in case of angular velocity sensor faults. In particular, each residual $r_{7,2}, ..., r_{15,2}$ (based on the SP approximated model, $n = 2$) is sensitive to the couple of physical faults $\mathbf{F_q}$, F_{ω_1}. On the other hand, each residual $r_{7,1}, ..., r_{15,1}$ (based on the exact model, $n = 1$) is sensitive to the physical fault $\mathbf{F_q}$ and a different couple of physical faults F_{ω_l} $(l = 1, ..., 3)$, *i.e.* to only one of the couples $\{F_{\omega_1}, F_{\omega_2}\}$, $\{F_{\omega_1}, F_{\omega_3}\}$, $\{F_{\omega_2}, F_{\omega_3}\}$.
(2) A faulty attitude sensor is isolated by checking if both sets have the same behaviour. Otherwise, a faulty angular velocity sensor is isolated by checking the residuals of the first set sensitive to each possible angular velocity sensor fault and by finding the three residuals sensitive only to the couple of not occurred sensor faults and not exceeding their thresholds.

Finally, due to the presence of measurement noise, residual thresholds have to be properly selected to achieve the best false alarm rate and missed fault rate performances.

4. SIMULATION RESULTS

The satellite body is modelled as a rectangular parallelepiped with dimensions 0.8 x 2.5 x 3 m, aerodynamic torque displacement vector $\mathbf{r_{cp}} = [0.10, 0.15, -0.25]$ m, drag coefficient $C_D = 2.2$, inertia values $I_{xx} = 330\,\mathrm{kg \cdot m^2}$, $I_{yy} = 150\,\mathrm{kg \cdot m^2}$, $I_{zz} = 140\,\mathrm{kg \cdot m^2}$. A flywheel moment of inertia $J_{rw} = 0.05\,\mathrm{kg \cdot m^2}$ and initial nominal flywheel spin rate values $\omega_0 = [3000, 3000, 3000]^T$ rpm for the three momentum wheels are assumed. The viscous and Coulomb friction parameters are $b = 5.16 \cdot 10^{-6}\,\mathrm{N \cdot m \cdot s}$ and $c = 0.8795 \cdot 10^{-3}\,\mathrm{N \cdot m}$, respectively. A circular orbit at an altitude of 350 km, with a null inclination and a low Earth equatorial orbit radius $R = 6728.140$ km, an atmosphere density $\rho = \rho_{mean} = 9.158 \cdot 10^{-12}\,\mathrm{kg/m^3}$, an orbital velocity $V = 8187.63$ m/s, and the Earth's gravitational constant $\mu = 39.86004418 \cdot 10^{13}\,\mathrm{m^3/s^2}$ is considered. Sensor noises are modelled by Gaussian processes with zero mean and standard deviations equal to 3 arcsec, 3 arcsec/s and 1 rpm for the attitude expressed in Euler angles, satellite angular velocity and flywheel spin rates, respectively. A simulation time of 60 s with a sampling time of 0.1 s is considered.
Assuming a single fault at any time, four additive fault scenarios commencing at $t_{fault} = 10$ s are considered:

(1) Actuator fault: $F_{M_2} = -a_M\,\omega_{rw_2}$ with a_M passing from zero at $t = 10$ s to 0.0001 Nms at $t = 12$ s;
(2) Flywheel sensor fault: $F_{\omega_{rw_2}} = -a_{\omega_{rw}}\,\omega_{rw_2} + b_{\omega_{rw}}$ with $a_{\omega_{rw}} = 0.05$, $b_{\omega_{rw}} = 0.3141$ rad/s $= 60$ rpm;
(3) Angular velocity sensor fault: $F_{\omega_3} = -a_\omega\,\omega_3 + b_\omega$ with $a_\omega = 0.05$, $b_\omega = -6.9808 \cdot 10^{-5}$ rad/s;
(4) Attitude sensor fault: $F_{\mathbf{q}}$ additive on the quaternion measurement, corresponding to a constant bias of -180 arcsec on the yaw angle measurements.

In case of the actuator fault F_{M_2}, Fig. 1 (a) shows the three diagnostic signals $r_1, ..., r_3$ provided by the NLGA residual filters based on the exact actuator model (6) and on the variables $\xi_1, ..., \xi_3$ (23) described in Section 3.5. These residual signals are exploited together with the three diagnostic signals $r_4, ..., r_6$ shown in Fig. 1 (b), which are provided by the NLGA residual filters based on the SP approximated model of the satellite dynamics (21) and on the variables $\xi_4, ..., \xi_6$ (24) described in Section 3.5, to detect and isolate the occurrence of actuator or flywheel spin rate sensor faults. The selected thresholds are depicted for each residual by means of red lines.
As described in Sections 3.5 and 3.8, each of the three residuals $r_1, ..., r_3$ is sensitive only to actuator and sensor faults possibly occurring on a specific momentum wheel subsystem, thus it is possible to detect and isolate the faulty subsystem just by means of these residuals. After the isolation of the faulty momentum wheel subsystem, a check on the three residuals $r_4, ..., r_6$ allows to precisely isolate also the type of the occurred fault since these

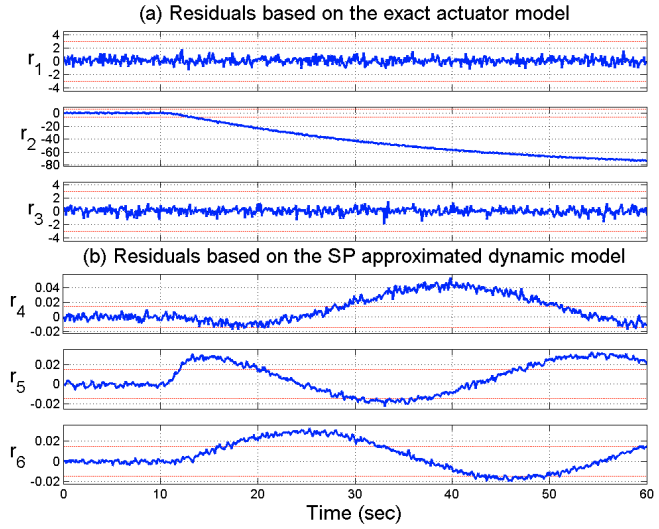

Fig. 1. Actuator fault: (a) three residuals based on the exact actuator model; (b) three residuals based on the SP approximated satellite dynamic model.

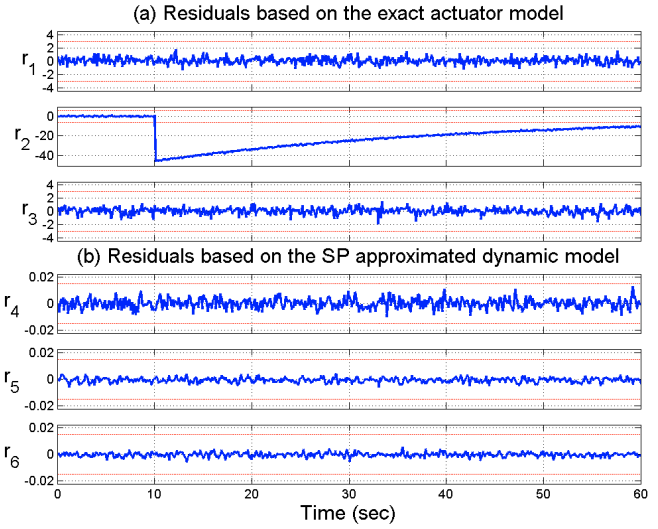

Fig. 2. Flywheel sensor fault: (a) three residuals based on the exact actuator model; (b) three residuals based on the SP approximated satellite dynamic model.

residuals are generally sensitive to any actuator faults and insensitive to any flywheel spin rate sensor faults.

It is worth noting that, in case of actuator fault, all the residuals $r_4, ..., r_6$ exceed their thresholds since the SP approximated dynamic model is an autonomous system without manipulable inputs, and it presents a significant error in the approximation of the actual satellite dynamics once the actual satellite equilibrium condition is lost due to the actuator fault occurrence.

In particular, the residual r_2 is sensitive to the couple of faults F_{M_2}, $F_{\omega_{rw_2}}$, whilst the diagnostic signals $r_4, ..., r_6$ are sensitive only to the actuator fault F_{M_2} and not to the sensor fault $F_{\omega_{rw_2}}$. In case of the actuator fault both r_2 and $r_4, ..., r_6$ exceed the selected thresholds. Hence, the occurred actuator fault F_{M_2} can be correctly isolated.

On the contrary, in case of the flywheel spin rate sensor fault $F_{\omega_{rw_2}}$, Fig. 2 (a) shows that the residual r_2 is sensitive to the occurred fault as in the previous case, but now the diagnostic signals $r_4, ..., r_6$ in Fig. 2 (b) do not exceed the selected thresholds after the sensor fault occurrence. Hence, the occurred flywheel sensor fault can be correctly isolated thanks to the different behaviour of the residuals.

Faults affecting the satellite angular velocity and attitude sensors can be detected and isolated by exploiting the two sets of nine diagnostic signals $r_{7,n}, ..., r_{15,n}$, $(n = 1, 2)$ provided by the NLGA residual filters based on the same set of nine variables $\xi_7, ..., \xi_{15}$ (24) described in Section 3.7. The first set $(n = 1)$ of residual filters has been designed using the exact kinematic model (2) of the satellite, whereas the second set $(n = 2)$ has been designed using the SP approximated kinematic model (25). Fig. 3 shows the residuals of the first $(n = 1)$ and second $(n = 2)$ set in case of the attitude sensor fault $\mathbf{F_q}$. As it can be seen, both sets are characterised by the same behaviours. Hence, an occurred attitude sensor fault can be easily detected and isolated as described in Section 3.8.

On the contrary, in case of the angular velocity sensor fault F_{ω_3}, the residuals of the two sets are characterised by different behaviours as shown in Fig. 4. In fact, since ω_2, ω_3 have been assumed as fast variables of the satellite dynamics, in the SP approximated model of the attitude kinematics these variables have been replaced with the obtained algebric solution of the manifold ω_{2M}, ω_{3M}, which does not depend on the actual value of the measured variables ω_2, ω_3. Therefore, the residuals of the second set $(n = 2)$ designed by exploiting the SP approximated model (25) are not sensitive to faults F_{ω_2}, F_{ω_3} on the corresponding sensors, as shown in Fig. 4 $(n = 2)$ where no residuals exceed their thresholds, while all of them are now sensitive to the fault F_{ω_1}. On the contrary, the residuals of the first set $(n = 1)$, which have been designed by means of the exact kinematic model (2), remain globally sensitive to all the angular velocity sensor faults, and in particular each of them to a specific couple of faults.

The occurrence of an angular velocity sensor fault can be recognized by cross-checking the corresponding residuals of the two sets as described in Section 3.8. If a different behaviour for any couple of corresponding residuals $r_{i,n}$ $(\forall i = 7, ..., 15$ and $n = 1, 2)$ is detected, it can be assumed that one of the sensor faults to which the two residuals are not both sensitive has occurred. For example, the residual $r_{7,1}$ is generally sensitive to the couple of faults F_{ω_2}, F_{ω_3} and in Fig. 4 it exceeds its threshold in case of the occurrence of F_{ω_3}. On the other hand, the residual $r_{7,2}$ based on the SP approximated model is sensitive only to the sensor fault F_{ω_1} and it does not exceed its threshold in case of the occurrence of F_{ω_3}. Hence, it can be stated that a fault F_{ω_2} or F_{ω_3} has occurred. Then, in order to accurately isolate the specific faulty sensor, the cross-check of the signals of the first set $(n = 1)$ can be performed on the basis of the decision logic described in Section 3.8. In fact, each NLGA residual filter of this set, which is based on the exact kinematic model of the satellite, results to be sensitive only to a specific couple of angular velocity sensor faults. In this case, the last three residuals $r_{13,1}, r_{14,1}, r_{15,1}$ of this set are decoupled from possible faults F_{ω_3} of the third angular velocity sensor and do not exceed their thresholds, in contrast with the other six residuals $r_{7,1}, r_{8,1}, r_{9,1}, r_{10,1}, r_{11,1}, r_{12,1}$, which are generally sensitive to the mathematical fault inputs associated to the occurred fault.

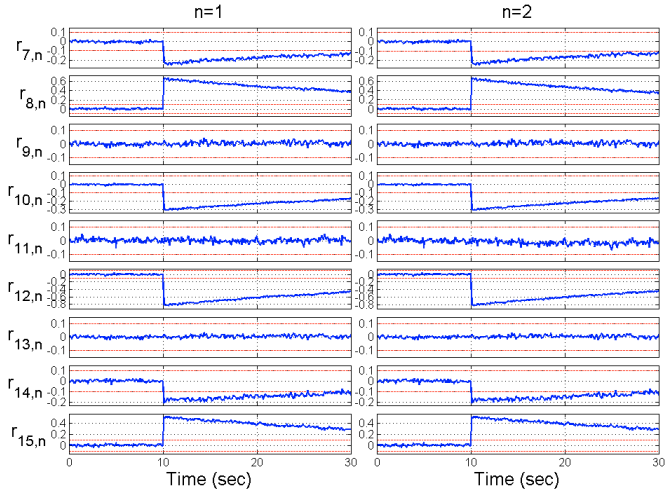

Fig. 3. Attitude sensor fault: sets of nine residuals based on the exact ($n = 1$) and SP approximated ($n = 2$) satellite kinematic model, respectively.

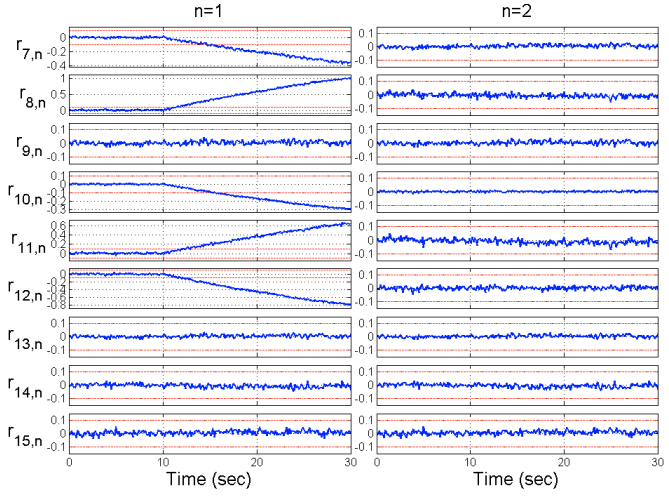

Fig. 4. Angular velocity sensor fault: sets of nine residuals based on the exact ($n = 1$) and SP approximated ($n = 2$) satellite kinematic model, respectively.

5. CONCLUSION

This paper presented a novel scheme for detection and isolation of actuator and sensor faults that affect the attitude determination and control system of a low Earth orbit satellite. The singular perturbation theory has been exploited to approximate the dynamics of the satellite characterised by different time scales. Thanks to jointly use of singular perturbations theory and nonlinear geometric approach, the developed system allows the accurate detection and isolation of faults occurring on all the actuators and sensors without requiring any additional hardware redundancy. Simulation results documented the effectiveness of the proposed scheme to achieve precise fault detection and isolation. Further developments will concern the implementation of the proposed scheme in fault diagnosis and fault-tolerant control systems.

REFERENCES

Baldi, P., Blanke, M., Castaldi, P., Mimmo, N., and Simani, S. (2016). Combined Geometric and Neural Network Approach to Generic Fault Diagnosis in Satellite Actuators and Sensors. *20th IFAC Symposium on Automatic Control in Aerospace - ACA 2016*, Sherbrooke (Canada), 49(17), 432–437.

Baldi, P., Castaldi, P., Mimmo, N., and Simani, S. (2014). A new aerodynamic decoupled frequential FDIR methodology for satellite actuator faults. *International Journal of Adaptive Control and Signal Processing*, 28(9), 812–832.

Blanke, M., Kinnaert, M., Lunze, J., and Staroswiecki, M. (2016). *Diagnosis and Fault–tolerant Control, 3rd Edition*. 3rd edition, Springer–Verlag Berlin Heidelberg.

Bokor, J. and Szabó, Z. (2009). Fault detection and isolation in nonlinear systems. *Annual Reviews in Control*, 33, 113–123.

Carrara, V., da Silva, A.G., and Kuga, H.K. (2012). A dynamic friction model for momentum wheels. *1st IAA Conference on Dynamic and Control of Space Systems*, 145, 343–352.

Castaldi, P., Mimmo, N., and Simani, S. (2014). Differential geometry based active fault tolerant control for aircraft. *Control Engineering Practice*, 32, 227–235.

Castaldi, P., and Mimmo, N. (2013). Aircraft nonlinear AFTC based on geometric approach and singular perturbations in case of actuator and sensor faults. *Proceedings of the 19th IFAC Symposium on Automatic Control in Aerospace - ACA 2013*, Wurzburg (Germany), 46(19), 30–35.

Castaldi, P., Geri, W., Bonf, M., Simani, S., and Benini, M. (2010). Design of residual generators and adaptive filters for the FDI of aircraft model sensors. *Control Engineering Practice*, 18(5), 449–459.

Chen, J., and Patton, R.J. (1999). *Robust Model–based Fault Diagnosis for Dynamic Systems*. Kluwer Ac. Publ.

De Persis, C., and Isidori, A. (2001). A geometric approach to nonlinear fault detection and isolation. *IEEE Transactions on Automatic Control*, 45, 853–865.

Ding, S.X. (2013). *Model–based Fault Diagnosis Techniques: Design Schemes, Algorithms, and Tools*. 2nd edition, Springer–Verlag London.

Isermann, R. (2011). *Fault Diagnosis Applications: Model–based Condition Monitoring: Actuators, Drives, Machinery, Plants, Sensors, and Fault-tolerant Systems*. Springer–Verlag Berlin Heidelberg.

Khalil, H.K. (2002). *Nonlinear Systems, 3rd Edition*. 3rd edition, Prentice Hall.

Mattone, R., and De Luca, A. (2006). Nonlinear fault detection and isolation in a three–tank heating system. *IEEE Transactions on Control Systems Technology*, 14(6), 1158–1166.

Simani, S., and Castaldi, P. (2014). Active actuator fault–tolerant control of a wind turbine benchmark model. *International Journal of Robust and Nonlinear Control*, 24(8–9), 1283–1303.

Wie, B. (2008). *Space Vehicle Dynamics and Control* (2nd ed.). AIAA Education Series.